Bromide Does Not Bind to the Mn_4Ca Complex in Its S_1 State in Cl^--Depleted and Br^--Reconstituted Oxygen-Evolving Photosystem II: Evidence from X-ray Absorption Spectroscopy at the Br K-Edge†

Michael Haumann,‡ Marcos Barra,‡ Paola Loja,‡ Simone Löscher,‡ Roland Krivanek,‡ Alexander Grundmeier,‡ Lars-Erik Andreasson,*,§ and Holger Dau*,‡

Freie Universität Berlin, FB Physik, Arnimallee 14, D-14195 Berlin, Germany, and Department of Chemistry, Division of Biochemistry and Biophysics, Göteborg University, P.O. Box 462, SE-405 30 Göteborg, Sweden

Received June 29, 2006; Revised Manuscript Received August 15, 2006

ABSTRACT: Chloride is an important cofactor in photosynthetic water oxidation. It can be replaced by bromide with retention of the oxygen-evolving activity of photosystem II (PSII). Binding of bromide to the Mn_4Ca complex of PSII in its dark-stable S_1 state was studied by X-ray absorption spectroscopy (XAS) at the Br K-edge in Cl^--depleted and Br^--substituted PSII membrane particles from spinach. The XAS spectra exclude the presence of metal ions in the first and second coordination spheres of Br^-. EXAFS analysis provided tentative evidence of at least one metal ion, which may be manganese or calcium, at a distance of ∼5 Å to Br^-. The native Cl^- ion may bind at a similar distance. Accordingly, water oxidation may not require binding of a halide directly to the metal ions of the Mn complex in its S_1 state.

The oxygen of the atmosphere is produced by the oxidation of two water molecules at the protein-bound manganese−calcium (Mn_4Ca) complex of photosystem II (PSII).[1] PSII is imbedded in the thylakoid membranes of green plants, algae, and cyanobacteria (*1*). Intensive research on this photosynthetic water oxidation has not led to a consensus about its mechanism. Oxygen evolution activity requires the presence of four Mn ions and one calcium per PSII reaction center, and maximal activity also requires chloride (*2*, *3*).

One calcium ion per PSII is essential for oxygen evolution as in its absence, activity is eliminated (*2*). The Ca^{2+} is ∼3.4 Å from two to three Mn ions (*4*−*7*). The location and functional role of chloride are less clear. A single Cl^- ion bound to PSII seems to be involved in oxygen evolution (*8*). If Cl^- removal is performed under conditions which lead to the partial release of the extrinsic polypeptides of PSII, activity may cease completely (refs *3* and *9* and references cited therein). However, the effect of Cl^- depletion is not always that severe. By dialysis of PSII membrane particles containing $^{36}Cl^-$ against Cl^--free medium, all Cl^- ions were removed, as verified by radiography, and the three extrinsic polypeptides remained bound (*8*). Such Cl^--depleted PSII preparations still exhibited an O_2 activity of ∼35% of the control. The activity was almost fully restored within seconds by the re-addition of either chloride or bromide (*8*−*10*). These results tentatively were interpreted as suggesting that Cl^- does not bind directly to Mn (*10*).

Recent crystallographic results for PSII from cyanobacteria have not provided indications for any halides in the vicinity of the manganese and/or calcium ions (*4*, *5*). On the other hand, X-ray absorption spectroscopy (XAS) data at the Mn K-edge of synthetic model compounds revealed that Mn−Cl interactions might contribute to the Mn XAS spectrum of PSII (ref *11* and references cited therein). However, if one of the 20−24 ligands of Mn were a halide, it would be difficult to resolve the corresponding contributions to the Mn XAS spectrum. Therefore, we employ an alternative approach. By XAS at the halide K-edge, we look for the presence of manganese and/or calcium in its first or higher coordination spheres.

A variety of modes of binding of Cl^- to the water-oxidizing complex has been discussed (Figure 1B−D) and crucial roles in the oxygen evolution chemistry proposed (see, e.g., refs *12*−*14*). In most of these models, Cl^- has been suggested to bind directly to the manganese and/or Ca^{2+} ions. XAS at the halide K-edge should be well suited to detect this binding mode since pronounced edge shape changes would be expected, as shown for model compounds with Cl^- ligated to manganese (*11*) or Br^- ligated to vanadium (*15*). Halide binding in higher coordination spheres of manganese or calcium may become detectable by EXAFS analysis. In a vanadium-dependent bromoperoxidase, Br^-

† Financial support from the Deutsche Forschungsgemeinschaft to H.D. and M.H. (Grants SFB498-C6 and -C8) and from the Swedish Science Council to L.-E.A. is gratefully acknowledged.

* To whom correspondence should be addressed. H.D.: FU Berlin, FB Physik, Arnimallee 14, D-14195 Berlin, Germany; phone, +49 30 8385 3581; fax, +49 30 8385 6299; e-mail, holger.dau@physik.fu-berlin.de. L.-E.A.: Department of Chemistry, Division of Biochemistry and Biophysics, Göteborg University, P.O. Box 462, SE-405 30 Göteborg, Sweden; phone, +46 31 773 3932; fax, +46 31 773 3910; e-mail, lars-erik.andreasson@chem.gu.se.

‡ Freie Universität Berlin.

§ Göteborg University.

[1] Abbreviations: chl, chlorophyll; DCBQ, dichloro-*p*-benzoquinone; DF, delayed chl fluorescence; EPR, electron paramagnetic resonance spectroscopy; EXAFS, extended X-ray absorption fine structure; fwhm, full width at half-maximum; MES, 2-morpholinoethanesulfonic acid; PSII, photosystem II; S_i, oxidation states in the S state cycle of water oxidation; TXRF, total reflection X-ray fluorescence analysis; XANES, X-ray absorption near-edge structure; XAS, X-ray absorption spectroscopy.

10.1021/bi061308r CCC: $33.50
Published on Web 10/04/2006

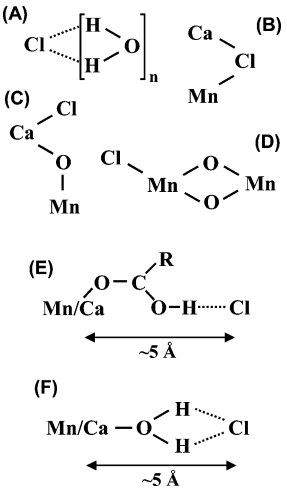

FIGURE 1: Suggested models for the binding of Cl^- to the Mn_4Ca complex of PSII. (A) Coordination of the Cl^- anion solely by bulk water molecules. The water protons and oxygens are in the first and second coordination spheres of Br^-, respectively. (B) Cl^- binding as a bridging ion between Mn and Ca^{2+} (*12*, *13*). (C) Cl^- as an end-on ligand to the Ca^{2+} ion bound via a bridging oxygen to Mn (*14*, *35*). (D) Cl^- as a terminal ligand to a di-μ-oxo-bridged Mn pair (*2*, *3*). (E and F) Possible binding modes of Cl^- or Br^- that are compatible with the Br XAS data in this investigation. The carboxylic amino acid, R, in panel E may correspond to D1-Asp170 of PSII. Further ligands to manganese and to the Ca^{2+} and Cl^- ions have been omitted for clarity.

binding has been characterized by XAS at the Br K-edge (*16*).

In this study, for the first time, X-ray absorption spectra at the Br K-edge were recorded for Cl^--depleted PSII membranes with the Mn complex in its S_1 state which had been reconstituted functionally with Br^-. In contrast to chlorine, bromine is very suitable for XAS studies because it absorbs at relatively high energies so that high-quality XAS spectra can be obtained even with micromolar concentrations of Br^- (weaker background absorption by water at higher energies). In addition, the natural abundance of Br^- is relatively low so that spurious contaminations could be excluded.

MATERIALS AND METHODS

PSII membranes were prepared from hydroponically grown spinach as described in ref *17* and frozen in liquid nitrogen until they were used. The oxygen evolution activity of PSII membranes was measured at 20 °C with a Clark-type oxygen electrode from Hansatech (*10*) with 1.25 mM phenyl-*p*-benzoquinone as an electron acceptor. The O_2 activity of the freshly prepared PSII membranes (no Cl^- depletion) was 650−700 μmol of O_2 (mg of chl)$^{-1}$ h^{-1} at saturating light intensity. Chloride was removed by repetitive washing followed by dialysis (Spectra/Por, molecular mass cutoff of 50 kDa) in the dark at 0 °C for 10 h against Cl^--free 20 mM MES-NaOH buffer (pH 6.3) with 1.4 M glycerol as a cryoprotectant as described in refs *8* and *10*. After Cl^- depletion and repletion with 25 mM NaCl, the activity of these control PSII samples was 550−600 μmol of O_2 (mg of chl)$^{-1}$ h^{-1} at saturating light intensity. The almost quantitative retention of the three extrinsic polypeptides of PSII with molecular masses of 18, 23, and 33 kDa in the Cl^--depleted samples was verified by gel electrophoresis (not shown). Cl^--depleted PSII membranes were suspended in 20 mM MES (pH 6.3) at a concentration of 0.5 mg of chl/mL at the NaBr concentrations given in the figures and incubated for 60 min on ice in darkness to allow binding of Br^- in the high-affinity mode (*9*, *10*). In these preparations, O_2 activities were measured at ~70% light saturation level to avoid photodamage of PSII (*8*, *10*).

Kinetic delayed chlorophyll fluorescence measurements (DF) were performed as described in ref *18*. Dark-adapted PSII samples (10 μg of chl/mL, 20 μM DCBQ added as an external electron acceptor) supplemented with the indicated Br^- concentrations were excited by trains of saturating flashes from a Continuum Minilite-II Laser (frequency-doubled, Q-switched Nd:YAG, $\lambda = 532$ nm, fwhm ~ 5 ns, flash spacing of 700 ms, 2 mJ/cm^2). Transients were recorded on a personal computer with a 20 MHz A/D card (Adlink) and in-house software using logarithmic spacing of data points starting 10 μs after the laser flash.

Control PSII membranes and Br^--substituted ones were concentrated by centrifugation to 16.5 mg of chl/mL (~65 μM PSII reaction centers on the basis of ~250 chl molecules/RC). The pellets were filled into acrylic−glass sample holders for XAS which were covered at the bottom side with Kapton foil and then frozen in liquid nitrogen. There was no Kapton on the side of the samples that was later exposed to the X-ray beam. All preparations and handling of PSII samples were carried out under dim green light to keep the Mn complex mainly in its dark-stable S_1 state. In the concentrated PSII samples, Br^- contents were quantified by the magnitude of the Br K-edge absorption in the XAS spectra and Br^- to Mn stoichiometries were determined by total reflection X-ray fluorescence (TXRF) analysis (*19*) on an instrument at Röntec (Berlin, Germany) using an aliquot of 5 μL from the original PSII XAS samples.

X-ray absorption spectroscopy (XAS) measurements at the Br K-edge were performed on two independent sets of samples during two measuring periods at bending-magnet beamline D2 of the Hamburg outstation of the European Molecular Biology Laboratory (EMBL) at HASYLAB (DESY, Hamburg, Germany) as described in refs *15* and *20*. By XAS measurements on PSII samples which were devoid of Br^-, it was verified that no significant Br^- contaminations were present in the beam. An absolute energy calibration was performed by the Bragg reflections method (*21*). The scan duration (13150−14150 eV) was ~30 min. Up to seven scans were performed on the same sample spot; no indications of radiation-induced modifications were detected. XAS spectra were normalized; 10−112 scans were averaged per spectrum, and EXAFS oscillations were extracted (*22*). The energy scale was transformed to a wavevector scale (k scale) using an E_0 of 13 474 eV. The k^3-weighted EXAFS oscillations were simulated using the in-house software SimX (*23*) and complex phase functions for different elements calculated with FEFF 7 (*24*). The amplitude reduction factor, S_0^2, was 0.9. The fit quality was judged by calculation of the Fourier-filtered R-factor (R_F) (*25*).

XANES simulations were performed with the ab initio code FEFF 8.2 (*26*) with both the full-multiple-scattering (FMS) and the self-consistent-field (SCF) options activated as outlined in ref *27*. Calculated XANES spectra were shifted by 4 eV to lower energies and multiplied by a factor of 1.05 for better comparison with the experimental spectra. Atomic

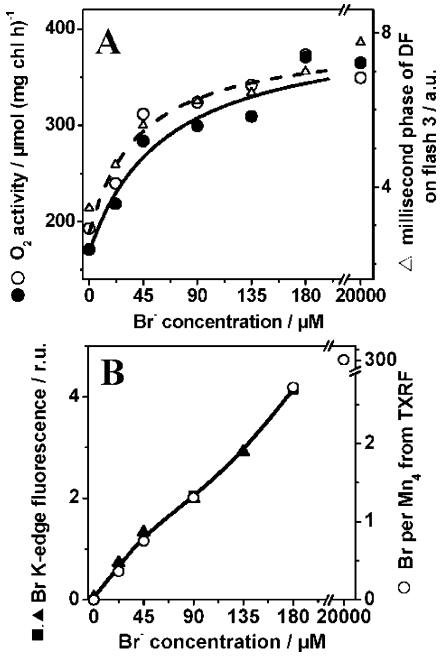

FIGURE 2: (A) Activation of Cl^--depleted PSII membranes with Br^-. PSII was depleted of Cl^-, incubated with Br^- at the indicated concentrations (see Materials and Methods), and assayed for O_2 activity in dialysis buffer at the same Br^- concentrations. The solid line represents a fit to the data (●) from samples for XAS (average of two data sets) using the Michaelis−Menten equation, where O_2 activity = O_2 activity$_{max}$[Br]/(K_D + [Br]) + offset, with a K_D of 53 μM and an offset activity of 160 μmol of O_2 (mg of chl)$^{-1}$ h^{-1}. A K_D of 43 μM (dashed line) was obtained from O_2 activities (○) and amplitudes of DF transients on flash 3 in the millisecond time range (△) in samples used for DF measurements. (B) Apparent Br^- content in PSII samples for XAS derived from the magnitude of the Br K-edge at 13480 eV [two independent data sets (■ and ▲); line, spline curve through the data points] and by TXRF (○). K-Edge magnitudes were normalized at the TXRF value at 90 μM Br^- for comparison.

coordinates for FEFF input files of XANES calculations were generated using Hyperchem 6 (Hypercube) and Br^-−ligand distances derived from the EXAFS simulations; the positions of atoms were optimized using the standard routines of Hyperchem.

RESULTS

The restoration of oxygen evolution activity in the Cl-depleted PSII membranes was assayed by polarography (Figure 2A). Compared to samples devoid of Cl^- and Br^-, these samples exhibited a pronounced gain in activity at low Br^- concentrations. The K_D value for Br^- was ∼53 μM in the samples later used for X-ray absorption analysis (●). The K_D and the absolute O_2 activity were found to be somewhat variable, depending on the preparation. A K_D of ∼43 μM (○) was obtained from the samples employed for chlorophyll fluorescence measurements (see below). We conclude that the K_D for binding of Br^- to PSII is in the range of 40−55 μM in our samples. At 180 μM Br^-, the activity was close to maximal, almost the same as with 20 mM Br^-, and ∼75% of that of a control sample (no previous Cl^- depletion, 20 mM Cl^- present). These results are comparable to earlier ones (*10*) and suggest that Br^- functionally substitutes for Cl^- in the major fraction of the PSII centers.

Flash-induced chlorophyll recombination fluorescence measurements [the so-called delayed fluorescence, DF (*18*)]

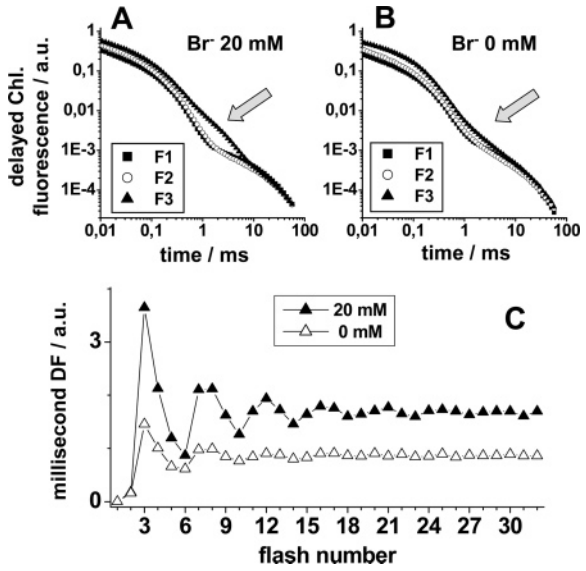

FIGURE 3: (A and B) Delayed chl fluorescence (DF) transients induced by the first three laser flashes (F1−F3) given to dark-adapted PSII samples supplemented with 20 mM and zero Br^-. The arrows mark the decay phase in the millisecond time range that can be attributed to oxygen release on flash 3. (C) Oscillation of the amplitude of the millisecond DF phase in a series of laser flashes at the two Br^- concentrations. Amplitudes have been obtained by a summation of the DF intensities in a time interval between 1 and 5 ms after the flashes (*28*).

were performed with Cl^--depleted and Br^--substituted PSII (Figure 3) to assess the initial S state composition of the samples. When 20 mM Br^- was present (Figure 3A, arrow), DF transients on the first three flashes from Cl^--depleted samples revealed a pronounced decay phase in the millisecond time range on flash 3, similar to a control sample (no previous Cl^- depletion, 20 mM Cl^- present, not shown). The millisecond phase seemingly was smaller in the absence of added Br^- (Figure 3B). Plotting the amplitudes of the millisecond phase against the added Br^- concentration [Figure 2A (△)] revealed the same K_D for Br^- binding (∼43 μM) that was obtained from the polarographic measurements. In a series of laser flashes, the amplitude of the millisecond phase, as determined by summation of the DF amplitudes in the time interval of 1−5 ms after the flash, showed a pronounced oscillation with a period of four and the first maximum occurring on flash 3 both with 20 mM and zero Br^- (Figure 3C). This behavior indicated (*28*) that most PSII centers were in the dark-stable S_1 state prior to flash 1. It should be noted that the DF amplitudes in Figure 3C depend on the time interval used for summation of fluorescence intensities. Different relative magnitudes of the DF on flash 3 in Cl^--depleted and Br^--substituted PSII are obtained if a different time interval is chosen, depending on the respective rate constants of the DF decay under the two conditions. A triple-exponential simulation (not shown; see ref *28*) of the DF transient on flash 3 in the sample with 20 mM Br^- revealed a half-time of O_2 evolution of 1.2 ms. Such a half-time is typical for intact PSII containing the three extrinsic polypeptides (*29*). In the absence of Br^-, the half-time was longer, namely, 2 ms, and the respective DF amplitude was ≤30% of that with 20 mM Br^-. (Kinetic components with longer decay times may be present but were not analyzed due to the limited time range of the measurements and due to the small fluorescence intensity at times

exceeding 10 ms.) These results are compatible with the notion that Br^- is bound to PSII already prior to flash 1 or becomes bound during the 700 ms time interval between flashes 1 and 2 or flashes 2 and 3.

The apparent content of Br^- of the PSII membrane samples used for XAS was monitored using the magnitude of the X-ray fluorescence at the Br K-edge (see below). Furthermore, the Br^- to Mn ratios and Cl^- contents were determined by TXRF. Figure 2B reveals that Br^- was not detectable in the Cl^--depleted PSII membranes which were not supplemented with exogenous Br^- (0 μM) by XAS and TXRF. In previous studies, it has been shown that the procedure used for Cl^- depletion results in completely Cl^--free samples (*8*). In the TXRF measurements, Cl^- was found to be below the detection limit (~0.1 Cl ion/Mn). By both detection methods, an increase in the Br^- content in the samples with an increasing amount of added Br^- was observed. The value determined by TXRF of 310 Br^- ions per four Mn atoms at 20 mM added Br^- was very compatible with the estimated concentration of ~65 μM PSII centers in the samples. On the basis of K_D values and PSII concentration, a reasonable estimate is that at ~34 μM Br, 40−50% of the Br^- in the samples functionally is bound to PSII (see the Supporting Information). At higher Br^- concentrations, the fraction of functionally bound Br^- is predicted to decrease continuously.

XANES spectra are particularly sensitive to changes in the first and second coordination spheres of Br^- (see Figure 1A) (*15*, *16*, *22*). Figure 4A shows that XANES spectra of PSII membranes supplemented with a substoichiometric Br^- concentration of 22 μM and with the excess concentration of 20 mM Br^- overall were similar. The spectrum of the 20 mM Br^- sample can largely be attributed to Br^- in solution where the first and second coordination spheres of the anion are occupied by protons and oxygen atoms, respectively, from water molecules (*15*, *16*, *30*), whereas the spectrum of the sample with 22 μM Br^- further may reflect changes in the coordination sphere of Br^- if it is bound to PSII. Indeed, there were subtle differences between the two spectra, e.g., a shift of the first EXAFS oscillation to lower energies (Figure 4A, inset) and a slightly sharper edge rise and an ~0.3 eV lower edge position (at 50% of the normalized fluorescence) of the spectrum from samples with 22 μM Br^- (~0.4 Br^- ion/4 Mn atoms) compared to that with 20 mM Br^- (~77 Br^- ions/4 Mn atoms).

Ab initio calculations of XANES spectra (*26*, *27*) were performed to estimate the effect of a slight increase in the Br−O distances and of a putative Mn or Ca ion ~5 Å from Br^- as found below in the EXAFS analysis (see the next section). The spectra which were calculated on the basis of the Br−ligand distances from the EXAFS analysis and using models **1** and **2** displayed in the figure are depicted in Figure 4B. The overall edge shape of the experimental spectra was reproduced, although we did not attempt to simulate the actual (but unknown) coordination geometry around the Br^- ion. The effect of the presence of a Mn or Ca ion 5 Å from the Br^- ion on the XANES spectrum was small. This result was anticipated because contributions of a metal at such a comparably large distance to the XAS spectrum predominantly are expected at the higher X-ray energies of the EXAFS region (see below). However, the slightly increased Br−O distances lead to a similar shift of the first EXAFS oscillation to lower energies in the calculated XANES spectrum (Figure 4B, inset) and to the steeper edge slope and lower edge energy as observed in the experimental spectrum from PSII samples. Thus, the changes in the XANES spectra likely are due to changes in the Br−O shell and are compatible with the notion that at 22 μM, Br^- is largely bound to PSII whereas at 20 mM, Br^- is located mainly in the bulk water phase.

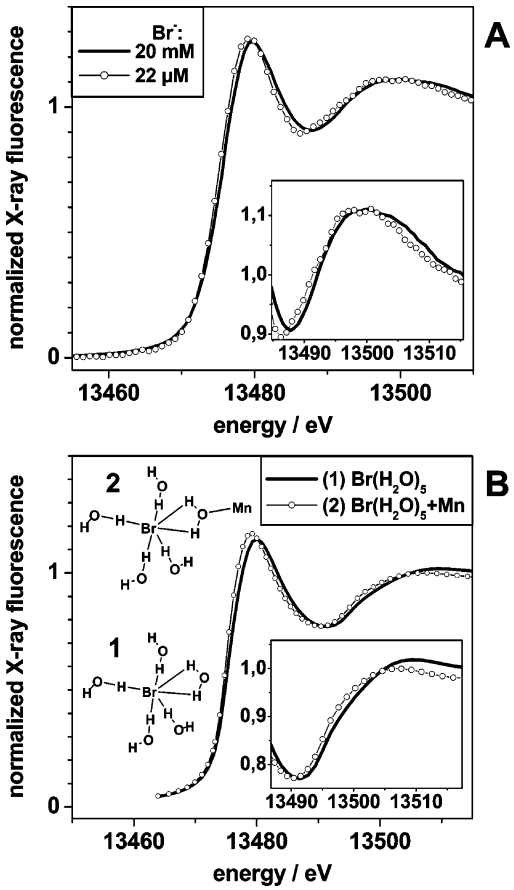

FIGURE 4: (A) XANES spectra collected at the Br K-edge for PSII membranes supplemented with the indicated Br^- concentrations. The inset shows an expansion of the spectra of samples with 20 mM (—) and 22 μM (○) Br^-. (B) XANES spectra calculated on basis of the model structures **1** and **2** and using the Br^-−ligand distances given in Table 1; the inset shows expanded spectra. The arrangement of the Br^- ligands in structures **1** and **2** is arbitrary.

Analysis of the EXAFS region of XAS spectra can be used to investigate whether metal ions are close to or farther from Br^-, up to ~5 Å (*22*). Figure 5A shows the Fourier transforms (FTs) of EXAFS oscillations of selected Br-substituted PSII samples. Clearly, there were differences in the shape of the FT of samples with 20 mM, 90 μM, and 34 μM Br^-. The magnitude of the prominent peak in the FT centered around reduced distances of ~2.8 Å was decreased at 34 and 90 μM Br^-. In the EXAFS spectrum of Br^- in solution (at 20 mM), this peak can be attributed to oxygen atoms in its second coordination sphere (Figure 1A) corresponding to Br−O distances of ~3.3 Å (*15*, *16*, *30*). Hence, the decrease in the magnitude of the respective FT peak suggests changes in the oxygen coordination sphere. (In PSII, there may be N or C atoms in the second coordination sphere of Br^- which are hard to distinguish from O.)

Simulation of the EXAFS spectrum of the samples with 20 mM Br^- employing one Br−O shell yielded a distance

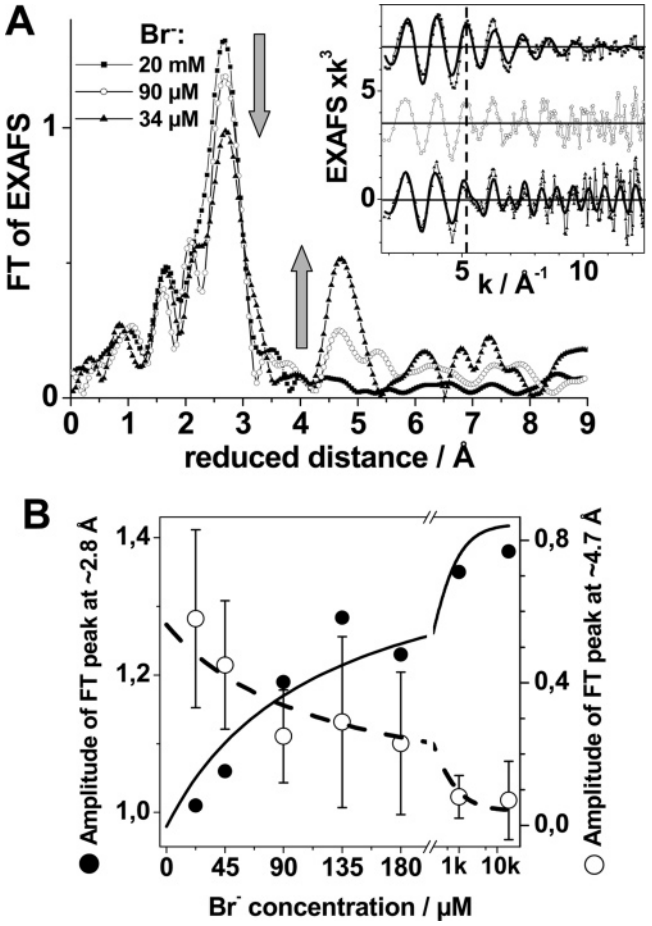

FIGURE 5: (A) Fourier transforms (FTs) of EXAFS oscillations of PSII particles supplemented with 34 μM (average of data from samples with 22 and 45 μM Br^-), 90 μM, and 20 mM Br^-. The arrows mark changes in the first and second relevant FT peaks. Data from four independent samples at each concentration which were obtained during two measuring periods at the synchrotron have been averaged. The inset shows the respective EXAFS oscillations (vertically displaced); the dashed line marks an EXAFS feature that changes with a decrease in Br^- concentration; solid lines show simulations with parameters given in Table 1. FTs were calculated for k values between 1.44 and 12.0 $Å^{-1}$ using fractional cosine windows over 25% at the high end and 10% at the low end of the k range. (B) Magnitudes of the FT peaks at ~2.8 (●) and ~4.7 Å (○) as a function of the Br^- concentration. Error bars represent a particularly stringent estimate of the noise level and correspond to the maximal magnitude of the respective FTs in the range of reduced distances of 6−9 Å, which are mainly attributable to noise contributions. Lines were calculated using eqs 3 (− − −) and 4 (−) in the Supporting Information and employing 65 μM PSII, a K_D of 53 μM, and appropriate scaling factors and offset values.

of 3.26 Å between the Br atom and the oxygen atoms in its second coordination sphere (Table 1), typical for Br^- ions in aqueous solution (*15*, *16*, *30*). It has been debated whether the protons in the first coordination shell of Br^- from ligating water molecules can be resolved by EXAFS (*16*). These protons may contribute to the shoulder at ~2.2 Å of the dominant FT peak at ~2.8 Å (Figure 3A). Here, we did not attempt to simulate such weak contributions to the EXAFS spectra. A simulation of the spectrum of the PSII samples containing a substoichiometric Br^- concentration of 34 μM revealed a slightly lower apparent coordination number of the Br−O shell and an ~0.04 Å longer mean Br−O distance of 3.30 Å (Table 1). Direct ligation of Br^- to Mn or Ca can be safely excluded. The change in the Br−O bond length likely is significant; the change in the coordination number may or may not be significant (estimated precision of ±20%). These results suggest that Br^- bound to PSII is no longer coordinated solely by water molecules of the bulk phase.

Table 1: Simulation Parameters of Br EXAFS Spectra (fit range 10−550 eV above E_0)[a]

sample	shell	N_i (per Br)	R_i (Å)	$2\sigma_i^2$ ($Å^2$)	R_F (%)
PSII plus 20 mM Br^-	Br···(H)−O	5.5	3.26	0.024	33.8
PSII plus 34 μM Br^-	Br···(H)−O	4.7	3.30	0.028	33.1
	Br···(H−O)···Mn/Ca	1.1	5.03	0.007	

[a] Here, N_i is the coordination number, R_i is the Br−backscatterer distance, $2\sigma_i^2$ is the Debye−Waller parameter, R_F is the error sum (*25*) calculated for reduced distances of 2−5.5 Å. E_0 refined to 13 486 eV in the fit procedure.

Interestingly, there is a second FT peak around 4.7 Å of reduced distance which increased in size for decreasing Br^- concentrations (Figure 5A, arrows). Figure 5B shows the magnitudes as a function of the Br^- concentration of the FT peaks at ~2.8 and ~4.7 Å. Apparently, the course of the increase of the ~2.8 Å peak and the decrease of the ~4.7 Å peak at increasing Br^- concentrations approximately followed the binding curve for binding of Br^- to PSII (Figure 5B, lines). The FT magnitude at ~4.7 Å at 34 μM Br^- is significantly larger than in the spectrum at 20 mM Br^-, a finding that cannot be explained by higher noise contributions. The EXAFS oscillations show larger magnitudes at higher k values in samples with micromolar Br^- concentrations than in samples with 20 mM Br^-, suggesting contributions from metal backscatterers at least in the sample with 34 μM Br^- (Figure 5A, inset). Simulation of the EXAFS oscillations of the sample with 34 μM Br^- was readily achieved employing one Br−O shell (see above) and, in addition, close to one Br−Mn/Ca vector 5.03 Å in length (Table 1). In summary, there is tentative evidence of the presence of at least one metal ion ~5 Å from Br^-.

DISCUSSION

In the Cl^--depleted PSII particles, the O_2 activity increased upon Br^- addition, showing a K_D of 40−55 μM. XAS spectra collected at the Br K-edge indicated binding of Br^- to the PSII particles. The Br^- concentration dependence is compatible with the same K_D for the observed XAS changes as for PSII functionalization by Br^- binding. This agreement provides evidence that the XAS-detectable changes are related to the functionalization of PSII by Br^- repletion.

Previous investigations have revealed various effects of Cl^- depletion on PSII. The $S_1 \rightarrow S_2$ transition of the water oxidation cycle still may function in Cl^--depleted PSII membranes, but oxidation of the Mn complex is blocked beyond the S_2 state (*31*); in Cl^--depleted PSII core particles, the Mn complex may be affected in the dark so that the first transition resembles the $S_2 \rightarrow S_3$ step in controls and Mn oxidation is largely blocked beyond S_3 (*32*). Cl^- depletion also seems to affect the S_2 state (*33*). These various effects may or may not be related to the use of different PSII preparations and to variations in the content of the extrinsic polypeptides. At least in Cl^--depleted PSII retaining the three extrinsic polypeptides, there seems to be significant residual O_2 activity (refs *8*−*10* and this work).

The XAS data collected at the Br K-edge exclude binding of Br^- as a first-sphere ligand to manganese or Ca^{2+} for the Mn complex in its S_1 state. The increase in the Br−O distances as observed at near-stoichiometric Br^- to Mn_4 ratios in this investigation suggests that Br^- and possibly also the native Cl^- ion bind to PSII already in the dark, when the Mn complex is in its S_1 state. The respective Br^- binding site may be ∼5 Å from a metal. This metal could be a manganese, meaning that Br^- may bind in its third to fifth coordination sphere. Alternatively, the metal ion might be the Ca^{2+} found ∼3.4 Å from Mn (*4*−*7*). Whether this binding site is the one that is relevant for the O_2-evolving step and whether the binding site changes upon transitions to higher S states remain to be elucidated.

The distance to manganese and to the Tyr-Z• radical (tyrosine 161 of the D1 protein) of various substances that may compete with Cl^- for its binding site has been investigated previously. Acetate is an inhibitor of oxygen evolution. Deuterons of methyl-deuterated acetate bound to PSII in the Tyr-Z• S_2 state have been proposed to be 3.1−6.1 Å from the nearest Mn atom, the range depending on the complexity of the model which was used to analyze the electron spin-echo envelope modulation (ESEEM) data (*36*), and 3.1 Å from the phenoxy oxygen of Tyr-Z• (*37*). Other authors also have reported evidence of binding of acetate close to Mn in the Tyr-Z• S_2 state (*38*, *39*). Azide may bind at a similar distance from Mn in the S_2 state of samples where Cl^- has been removed by dialysis (*40*). Whether the binding site of these inhibitors is the same as that of Cl^- or Br^- remains to be shown. The estimated range of distances between acetate and the Mn complex in its S_2 state is similar to the Br^-−Mn distance which is compatible with our XAS results and could suggest a comparable Mn−Cl^- distance in S_2 and S_1. Further investigations are required to clarify these issues.

The question of whether a Br−Mn or Br−Ca distance of ∼5 Å suggests binding of the native Cl^- ion at a similar distance from the metal(s) emerges. In the crystal structures, there was no evidence of halides in the vicinity of the Mn complex (*4*, *5*). However, the relatively small Cl^- ion, if it was somewhat disordered, may have escaped detection at the current resolution of 3.0 Å (*5*). The ionic radius of Cl^- is 1.81 Å, compared to a radius of 1.96 Å for Br^- (*34*). The comparable radius of Cl^- may allow it to bind to Mn or Ca at a distance similar to that for Br^-. In conclusion, our results do not support options B−D in Figure 1 (i.e., Cl^- as a first-sphere ligand to Mn or Ca^{2+}) but rather options E and F (Cl in the third to fifth coordination sphere) at least in the S_1 state.

At present, the nature of the Cl^- and Br^- binding sites in PSII is unknown. We obtained evidence that there are differences in the oxygen (or nitrogen/carbon) shell of Br^- bound to PSII membranes compared to its coordination in water. The respective O, N, and C ligands may stem from amino acid residues and/or from water molecules in the protein. Possible binding modes of Cl^- or Br^- in the vicinity of the Mn/Ca complex are depicted in Figure 1E,F. In the crystal structures of PSII, there is apparently unassigned space in the vicinity of the Mn complex around residue D1-Asp170 which appears to be a monodentate Mn ligand (*4*, *5*). A binding mode of the Cl^- ion as depicted in Figure 1E thus may be realized, e.g., by its binding to D1-Asp170 and possibly involving CP43-Arg357 in addition (*13*, *41*).

Conceivable functions of Cl (Br^-) in water oxidation include adjustment of the redox potential of the Mn complex, participation in proton transfer from bound water, maintaining the structural integrity of the active site, and positioning of the substrate water molecules (see refs *2*, *3*, *8*−*10*, and *12*−*14* and Figure 1). A distance between the Cl^- anion and the Mn complex of ∼5 Å may be compatible with either of these functions. Residue D1-Asp61 has been proposed to be at the entrance of a proton channel from the Mn complex to the bulk (*4*). Binding of Cl^- close to D1-Asp170 as discussed above thus may suggest a role in proton transfer from the site of water oxidation to the bulk as previously proposed (*10*). More specific attributions require further structural investigations to unravel the precise binding mode of Cl^- or Br^- within PSII.

ACKNOWLEDGMENT

We thank Dr. W. Meyer-Klaucke at EMBL (Hamburg outstation) for excellent support, Dr. H. Stosnach from Röntec for generous help with the TXRF measurements, and H. Andersson (Göteborg University) for skillful assistance in the PSII preparations.

SUPPORTING INFORMATION AVAILABLE

An estimation of the amount of Br^- bound to PSII and one table. This material is available free of charge via the Internet at http://pubs.acs.org.

REFERENCES

1. Nugent, J. H. A., Ed. (2001) Special Issue on Photosynthetic Water Oxidation, *Biochimica et Biophysica Acta*, Vol. 1503, Elsevier, Amsterdam.
2. Debus, R. J. (1992) The manganese and calcium ions of photosynthetic oxygen evolution, *Biochim. Biophys. Acta 1102*, 269−352.
3. Yocum, C. F. (1992) The calcium and chloride ions in photosynthetic water oxidation, in *Manganese Redox Enzymes* (Pecoraro, V. L., Ed.) pp 71−83, VCH, New York.
4. Ferreira, K. N., Iverson, T. M., Maghlaoui, K., Barber, J., and Iwata, S. (2004) Architecture of the photosynthetic oxygen-evolving center, *Science 303*, 1831−1838.
5. Loll, B., Kern, J., Saenger, W., Zouni, A., and Biesiadka, J. (2005) Towards complete cofactor arrangement in the 3.0 Å resolution structure of photosystem II, *Nature 438*, 1040−1044.
6. Cinco, R. M., McFarlane Holman, K. L., Robblee, J. H., Yano, J., Pizarro, S. A., Bellacchio, E., Sauer, K., and Yachandra, V. K. (2002) Calcium EXAFS establishes the Mn−Ca cluster in the oxygen-evolving complex of Photosystem II, *Biochemistry 41*, 12928−12933.
7. Müller, C., Liebisch, P., Barra, M., Dau, H., and Haumann, M. (2005) The location of calcium in the manganese complex of oxygenic photosynthesis studied by X-ray absorption spectroscopy, *Phys. Scr. T115*, 847−850.
8. Lindberg, K., Wydrzynski, T., Vänngard, T., and Andreasson, L.-E. (1990) Slow release of chloride from ^{36}Cl-labeled photosystem II membranes, *FEBS Lett. 264*, 153−155.
9. Lindberg, K., and Andreasson, L.-E. (1996) A one-site, two-state model for the binding of anions in photosystem II, *Biochemistry 35*, 14259−14267.
10. Olesen, K., and Andreasson, L.-E. (2003) The function of the chloride ion in photosynthetic oxygen evolution, *Biochemistry 42*, 2025−2035.
11. Pizarro, S. A., Visser, H., Cinco, R. M., Robblee, J. H., Pal, S., Mukhopadhyay, S., Mok, H. J., Sauer, K., Wieghardt, K., Armstrong, W. H., and Yachandra, V. K. (2004) Chloride ligation

in inorganic manganese model compounds relevant to photosystem II studied using X-ray absorption spectroscopy, *J. Biol. Inorg. Chem. 9*, 247−255.
12. Vrettos, J. S., Limburg, J., and Brudvig, G. W. (2001) Mechanism of photosynthetic water oxidation: Combining biophysical studies of photosystem II with inorganic model chemistry, *Biochim. Biophys. Acta 1503*, 229−245.
13. McEvoy, J. P., and Brudvig, G. W. (2004) Structure-based mechanism of photosynthetic water oxidation, *Phys. Chem. Chem. Phys. 6*, 4754−4763.
14. Tommos, C., and Babcock, G. T. (1998) Oxygen production in nature: A light metalloradical enzyme process, *Acc. Chem. Res. 31*, 18−25.
15. Dau, H., Dittmer, J., Epple, M., Hanss, J., Kiss, E., Rehder, D., Schulzke, C., and Vilter, H. (1999) Bromine K-edge EXAFS studies of bromide binding to bromoperoxidase from *Ascophyllum nodosum*, *FEBS Lett. 457*, 237−240.
16. Rehder, D., Schulzke, C., Dau, H., Meinke, C., Hanss, J., and Epple, M. (2000) Water and bromide in the active center of vanadate-dependent haloperoxidases, *J. Inorg. Biochem. 80*, 115−121.
17. Franze, L. G., Hansson, O., and Andreasson, L.-E. (1985) The roles of the extrinsic subunits in Photosystem II as revealed by EPR, *Biochim. Biophys. Acta 808*, 171−179.
18. Grabolle, M., and Dau, H. (2005) Energetics of primary and secondary electron transfer in photosystem II membrane particles of spinach revisited on basis of recombination-fluorescence measurements, *Biochim. Biophys. Acta 1708*, 209−218.
19. Klockenkämper, R. (1996) *Total Reflection X-ray Fluorescence Analysis*, Wiley, London.
20. Iuzzolino, L., Dittmer, J., Dörner, W., Meyer-Klaucke, W., and Dau, H. (1998) X-ray absorption spectroscopy on layered photosystem II membrane particles suggests manganese-centered oxidation of the oxygen-evolving complex for the S0−S1, S1−S2, and S2−S3 transitions of the water oxidation cycle, *Biochemistry 37*, 17112−17119.
21. Pettifer, R. F., and Hermes, C. (1985) Absolute energy calibration of X-ray radiation from synchrotron sources, *J. Appl. Crystallogr. 18*, 404−412.
22. Dau, H., Liebisch, P., and Haumann, M. (2003) X-ray absorption spectroscopy to analyze nuclear geometry and electronic structure of biological metal centers: Potential and questions examined with special focus on the tetranuclear manganese complex of oxygenic photosynthesis, *Anal. Bioanal. Chem. 376*, 562−583.
23. Dittmer, J. (1999) Röntgenabsorptionsspektroskopie zum katalytischen Zyklus des wasserspaltenden Mangankomplexes der Photosynthese in Theorie und Experiment, Ph.D. Thesis, Christian Albrechts Universität Kiel, Kiel, Germany.
24. Rehr, J. J., Mustre de Leon, J., Zabinsky, S. I., and Albers, R. C. (1991) Theoretical X-ray absorption fine structure standards, *J. Am. Chem. Soc. 113*, 5135−5140.
25. Meinke, C., Sole, V. A., Pospisil, P., and Dau, H. (2000) Does the structure of the water-oxidizing photosystem II-manganese complex at room temperature differ from its low-temperature structure? A comparative X-ray absorption study, *Biochemistry 39*, 7033−7040.
26. Ankudinov, A. L., Ravel, B., Rehr, J. J., and Conradson, S. D. (1998) Real-space multiple-scattering calculation and interpretation of X-ray-absorption near-edge structure, *Phys. Rev. B 58*, 7565−7576.
27. Burgdorf, T., Loscher, S., Liebisch, P., Van der Linden, E., Galander, M., Lendzian, F., Meyer-Klaucke, W., Albracht, S. P., Friedrich, B., Dau, H., and Haumann, M. (2005) Structural and oxidation-state changes at its nonstandard Ni−Fe site during activation of the NAD-reducing hydrogenase from *Ralstonia eutropha* detected by X-ray absorption, EPR, and FTIR spectroscopy, *J. Am. Chem. Soc. 127*, 576−592.
28. Clausen, J., Junge, W., Dau, H., and Haumann, M. (2005) Photosynthetic water oxidation at high O_2 backpressure monitored by delayed chlorophyll fluorescence, *Biochemistry 44*, 12775−12779.
29. Haumann, M., Hundelt, M., Jahns, P., Chroni, S., Bögershausen, O., Ghanotakis, D., and Junge, W. (1997) Proton release from water oxidation by photosystem II: Similar stoichiometries are stabilized in thylakoids and core particles by glycerol, *FEBS Lett. 410*, 243−248.
30. Feiters, M., Küpper, F. C., and Meyer-Klaucke, W. (2005) X-ray absorption spectroscopic studies on model compounds for biological iodine and bromine, *J. Synchrotron Radiat. 12*, 85−93.
31. Wincencjusz, H., van Gorkom, H. J., and Yocum, C. F. (1997) The photosynthetic oxygen evolving complex requires chloride for its redox state S2 → S3 and S3 → S0 transitions but not for S0 → S1 or S1 → S2 transitions, *Biochemistry 36*, 3663−3670.
32. Haumann, M., Drevenstedt, W., Hundelt, M., and Junge, W. (1997) Photosystem II of green plants: Oxidation and deprotonation of the same component (Histidine?) on S_1^* → S_2^* in chloride depleted centers as on S_2 → S_3 in controls, *Biochim. Biophys. Acta 1273*, 237−250.
33. Van Vliet, P., and Rutherford, A. W. (1996) Properties of the chloride-depleted oxygen-evolving complex of photosystem II studied by electron paramagnetic resonance, *Biochemistry 35*, 1829−1839.
34. Shannon, R. D. (1976) Revised effective ionic radii and systematic studies of interatomic distances in halides and chalcogenides, *Acta Crystallogr. A32*, 751−767.
35. Robblee, J. H., Cinco, R. M., and Yachandra, V. K. (2001) X-ray spectroscopy-based structure of the Mn cluster and mechanism of photosynthetic oxygen evolution, *Biochim. Biophys. Acta 1503*, 7−23.
36. Clemens, K. L., Force, D. A., and Britt, R. D. (2002) Acetate binding at the photosystem II oxygen evolving complex: An S_2-state multiline ESEEM study, *J. Am. Chem. Soc. 124*, 10921−10933.
37. Force, D. A., Randall, D. W., and Britt, R. D. (1997) Proximity of acetate, manganese, and exchangeable deuterons to tyrosine $Y_Z^\bullet$ in acetate-inhibited photosystem II membranes: Implications for the direct involvement of $Y_Z^\bullet$ in water-splitting, *Biochemistry 36*, 12062−12070.
38. Szalai, V. A., and Brudvig, G. W. (1996) Reversible binding of nitric oxide to tyrosyl radicals in photosystem II. Nitric oxide quenches formation of the S3 EPR signal species in acetate-inhibited photosystem II, *Biochemistry 35*, 15080−15087.
39. Kühne, H., Szalai, V. A., and Brudvig, G. W. (1999) Competitive binding of acetate and chloride in photosystem II, *Biochemistry 38*, 6604−6613.
40. Yu, H., Aznar, C. P., Xu, X., and Britt, R. D. (2005) Evidence that azide occupies the chloride binding site near the manganese cluster in photosystem II, *Biochemistry 44*, 12022−12029.
41. Haumann, M., Liebisch, P., Müller, C., Barra, M., Grabolle, M., and Dau, H. (2005) Photosynthetic O_2 formation tracked by time-resolved X-ray experiments, *Science 310*, 1019−1021.

BI061308R